Supporting Information

Adsorption Characteristics of Metal Organic Frameworks containing Coordinatively Unsaturated Metal Sites: Effect of Metal Cations and Adsorbate Properties

*Prashant Mishra, Satyannarayana Edubilli, Bishnupada Mandal, Sasidhar Gumma**

Department of Chemical Engineering, Indian Institute of Technology Guwahati
Guwahati - 781039, Assam, India.

Contents

Page S2. Physical properties of gases.

Page S3-S4. Synthesis.

Page S5-S6. Material characterization.

Page S7-S24. Adsorption isotherms.

Page S25-S27. Fit parameters.

Page S28. Adsorption Enthalpies.

Page S29-S30. IAST predictions.

Page S31. References.

Table S1. Physical properties of studied gases.

gas	molecular Weight (g mol^{-1})	kinetic diameter (Å)	polarizability ($\times 10^{-25}$ cm^3)	quadrupole moment ($\times 10^{-40}$ C*m^2)	dipole moment ($\times 10^{18}$ esu.cm)
CO_2	44	3.3	26.3	14.3	0.0
CO	28	3.76	19.5	2.5	0.112
CH_4	16	3.8	26.0	0.0	0.0
C_2H_6	30	4.4	44.7	0.65	0.0
N_2	28	3.64	17.6	1.52	0.0
Ar	40	3.4	16.6	0.0	0.0

Synthesis

Mg/DOBDC. The synthesis was carried out as per procedure suggested by Caskey et al.[1] A solid mixture of 2,5-dihydroxy terephthalic acid (0.888 g, 4.472 mmol, Sigma aldrich) and $Mg(NO_3)_2 \cdot 6H_2O$ (3.795 g, 14.8 mmol, Merck) was added into a 15:1:1 (v/v/v) mixture of DMF/ethanol/water (400 mL). The suspension was sonicated for about 5 minutes to make it homogeneous. Then the suspension was equally distributed in twenty seven 30-mL polypropylene vials. These vials were capped tightly and kept in an oven at 398 K for 20 hours. Samples were then cooled to RT followed by decantation of mother liquid from obtained yellowish crystals. Methanol of similar quantity as of mother liquid (~15 mL per vials) was added. Then suspension was collected in one 500-mL polypropylene vial. After every 12 hours, methanol was decanted and replaced with fresh one for two days to get as-synthesized Mg/DOBDC crystals. These crystals were dried and stored in vacuum.

Co/DOBDC. As per procedure suggested elsewhere[1] 2,5-dihydroxy terephthalic acid (0.482 g, 2.43 mmol, Sigma aldrich), $Co(NO_3)_2 \cdot 6H_2O$ (2.377 g, 8.67 mmol, Merck) and a 1:1:1 (v/v/v) mixture of DMF–ethanol–water (200 mL) were mixed in a 500 ml polypropylene vial. Sonication of the suspension was done for about 5 minutes to make it homogeneous. Then vial was capped tightly and kept in an oven at 373 K for 24 hours. Sample was then cooled to RT followed by decantation of mother liquid from obtained crystals. Methanol of similar quantity as of mother liquid (~200 mL) was added. After every 12 hours, methanol was decanted and replaced with fresh one for two days to get as-synthesized Co/DOBDC crystals of violet color. These crystals were dried and stored in vacuum.

Ni/DOBDC. The synthesis was carried out as per procedure suggested by Caskey et al.[1] A solid mixture of 2,5-dihydroxy terephthalic acid (0.478 g, 2.41 mmol, Sigma aldrich) and $Ni(NO_3)_2 \cdot 6H_2O$ (2.378 g, 8.178 mmol, Merck) were added to a 1:1:1 (v/v/v) mixture of DMF–ethanol–water (200 mL) in a 500 ml polypropylene vial. Sonication of the suspension was done for about 5 minutes to make it homogeneous. Then vial was capped tightly and kept in an oven at 373 K for 24 hours. Sample was then cooled to RT followed by decantation of mother liquid from obtained crystals. Methanol of similar quantity as of mother liquid (~200 mL) was added. After every 12 hours, methanol was decanted and replaced with fresh one for two days to get as-synthesized Ni/DOBDC crystals of yellowish green color. These crystals were dried and stored in vacuum.

Mn/DOBDC. Synthesis procedure was slightly modified from that reported in literature.[2] A solid mixture of 2,5-dihydroxy terephthalic acid (0.888 g, 4.472 mmol, Sigma aldrich) and $Mn(NO_3)_2 \cdot 4H_2O$ (3.715 g, 14.8 mmol, Merck) was added into a 15:1:1 (v/v/v) mixture of DMF/ethanol/water (400 mL). The suspension was sonicated for about 5 minutes to make it homogeneous. Then the suspension was equally distributed in twenty seven 30-mL polypropylene vials. These vials were capped tightly and kept in an oven at 404 K for 24 hours. Samples were then cooled to RT followed by decantation of mother liquid from obtained brownish crystals. Methanol of similar quantity as of mother liquid (~15 mL per vials) was added. Then suspension was collected in one 500-mL polypropylene vial. After every 12 hours, methanol was decanted and replaced with fresh one for two days to get as-synthesized Mn/DOBDC crystals. These crystals were dried and stored in vacuum.

Material Characterization

Thermogravimetric analysis (TGA). TGA of all M/DOBDC samples (M = Mg, Mn, Co and Ni) was performed in a thermogravimetric analyzer (Mettler TOLEDO, model no. TGA/SDTA 851^{e}). The temperature was ramped from 298 to 873 K with a heating rate of 5 K min^{-1}, and the measurements were carried out under a nitrogen atmosphere. The results are given in Figure S1. There are total three weight loss steps for each sample. First weight loss step up to 377 K is relatively rapid, and corresponds to removal solvent (methanol) and moisture. Second slack weight loss is due to detachment of coordinatively bonded water molecules; thus creating coordinatively unsaturated metal sites in the frameworks.[3] Start of the final weight loss step corresponding to the decomposition of the sample and collapse of the framework structure varies for different sample; it started at the highest temperature (~700 K) for Mg/DOBDC and at lowest temperature (~560 K) for Co/DOBDC.

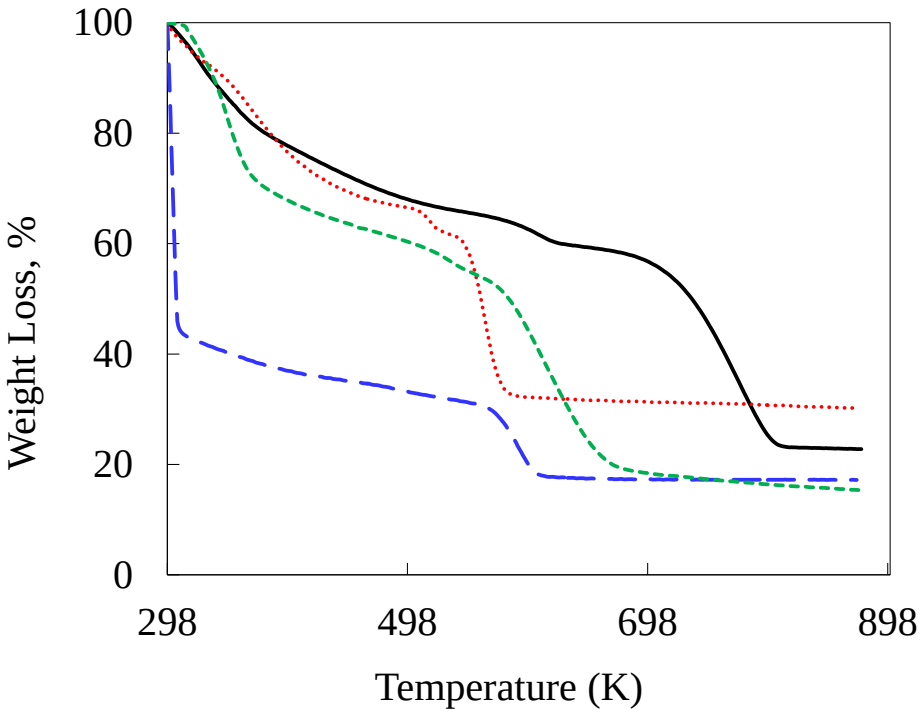

Figure S1. TGA analysis of Mg/DOBDC (—), Mn/DOBDC (---), Co/DOBDC (⋯) and Ni/DOBDC (– –) at heating rate of 5 K min^{-1} under flow of N_2.

X-ray diffraction (XRD) analysis. XRD analysis of synthesis M/DOBDC samples was carried on a Bruker A8 advance instrument operating at 40 kV and 40 mA using Cu Kα (λ = 1.5406 Å) radiation. The powder X-ray diffraction (XRD) patterns (Figure S2) are similar to the XRD pattern reported for these materials in the literature.[2]

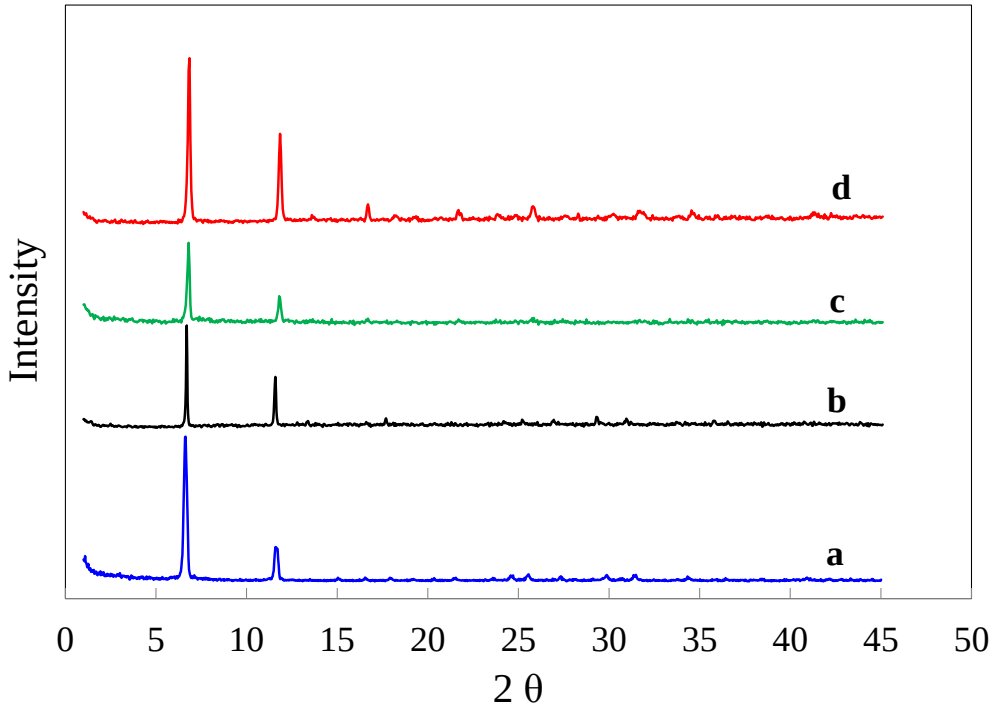

Figure S2. X-ray diffractogram of (a) Mg/DOBDC, (b) Mn/DOBDC, (c) Co/DOBDC and (d) Ni/DOBDC.

Adsorption isotherms-

Multi-temperature adsorption isotherms of different adsorbates

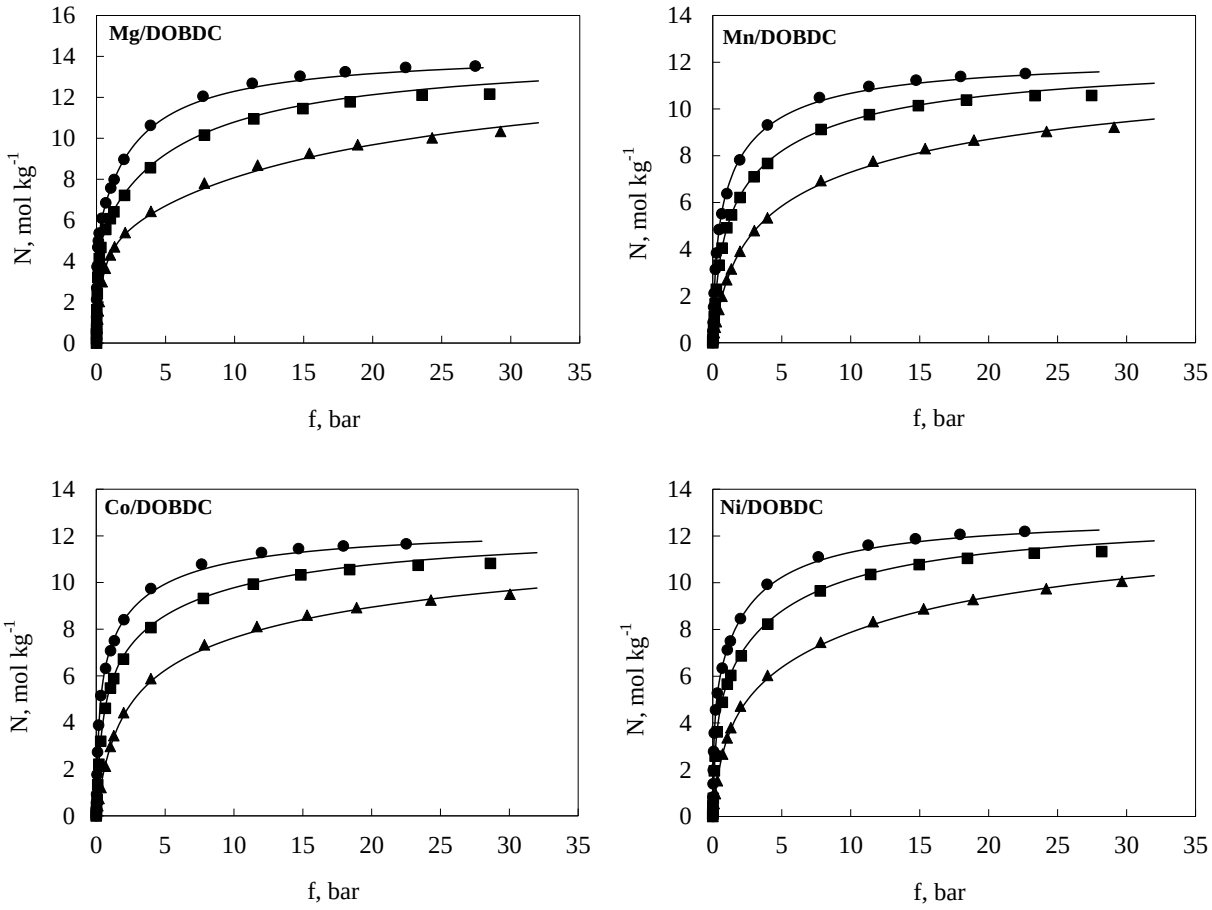

Figure S3. CO_2 isotherms. Symbols are experimental data at 294 K (●), 315 K (■) and 352 K (▲); lines are fits obtained using DSL isotherm parameters from Tables S2.

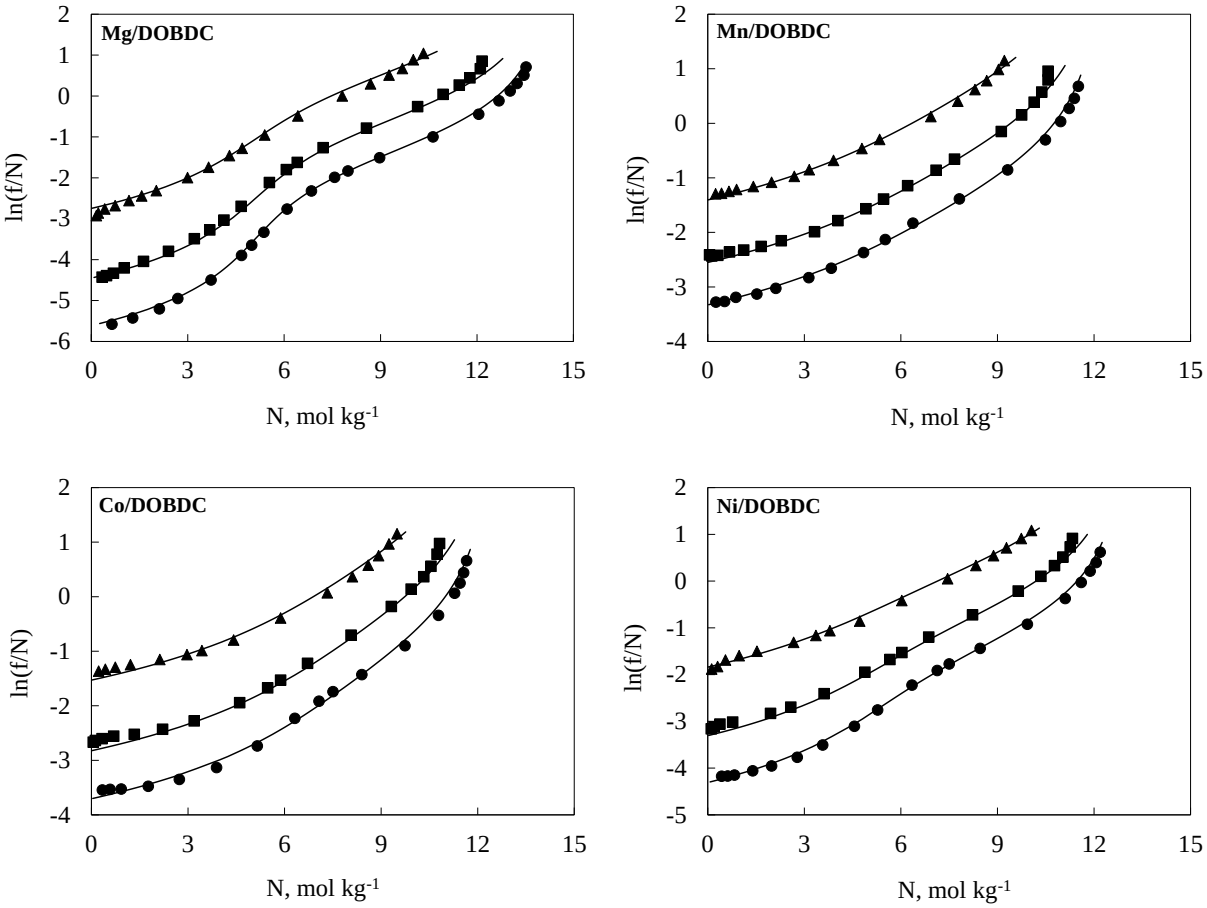

Figure S4. CO_2 isotherms in virial domain. Symbols are experimental data at 294 K (●), 315 K (■) and 352 K (▲); lines are fits obtained using DSL isotherm parameters from Tables S2.

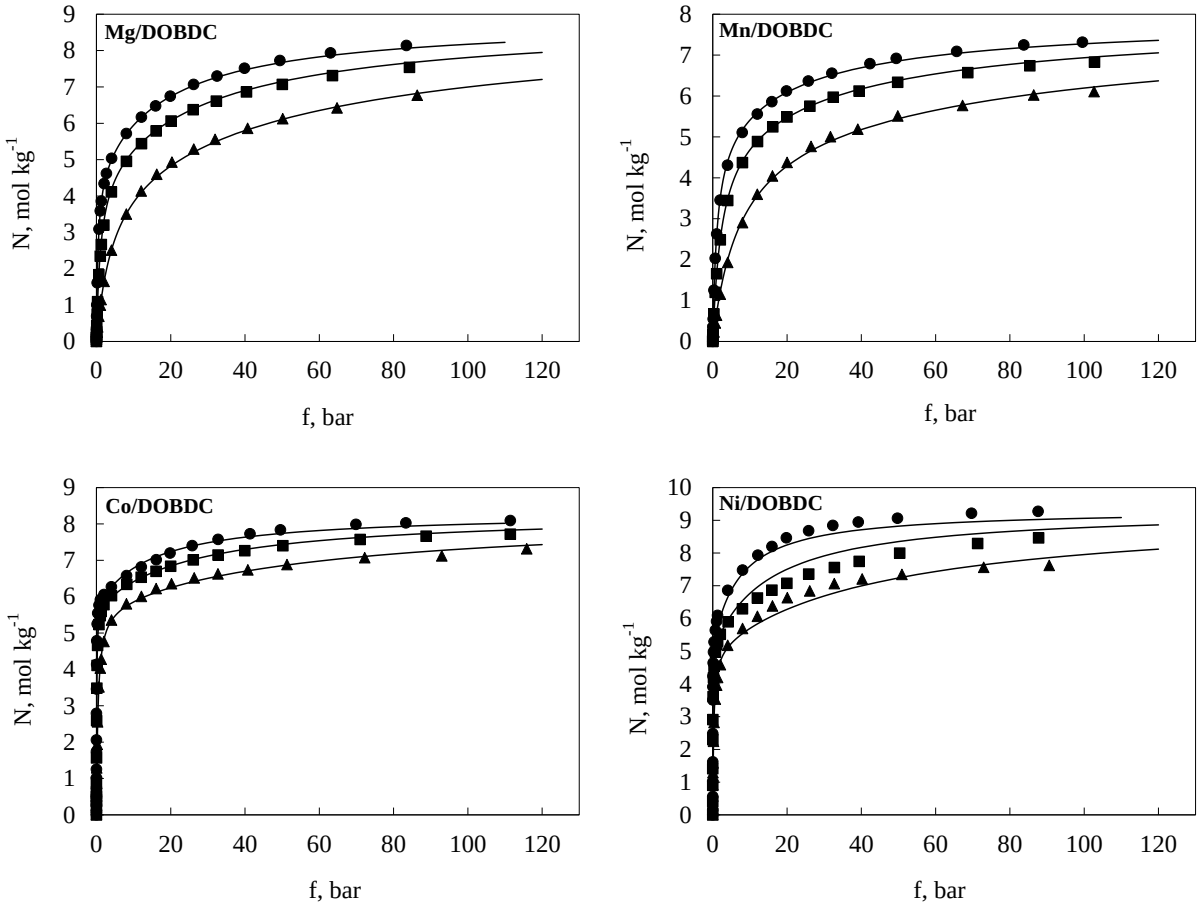

Figure S5. CO isotherms. Symbols are experimental data at 294 K (●), 315 K (■) and 352 K (▲); lines are fits obtained using DSL isotherm parameters from Tables S3.

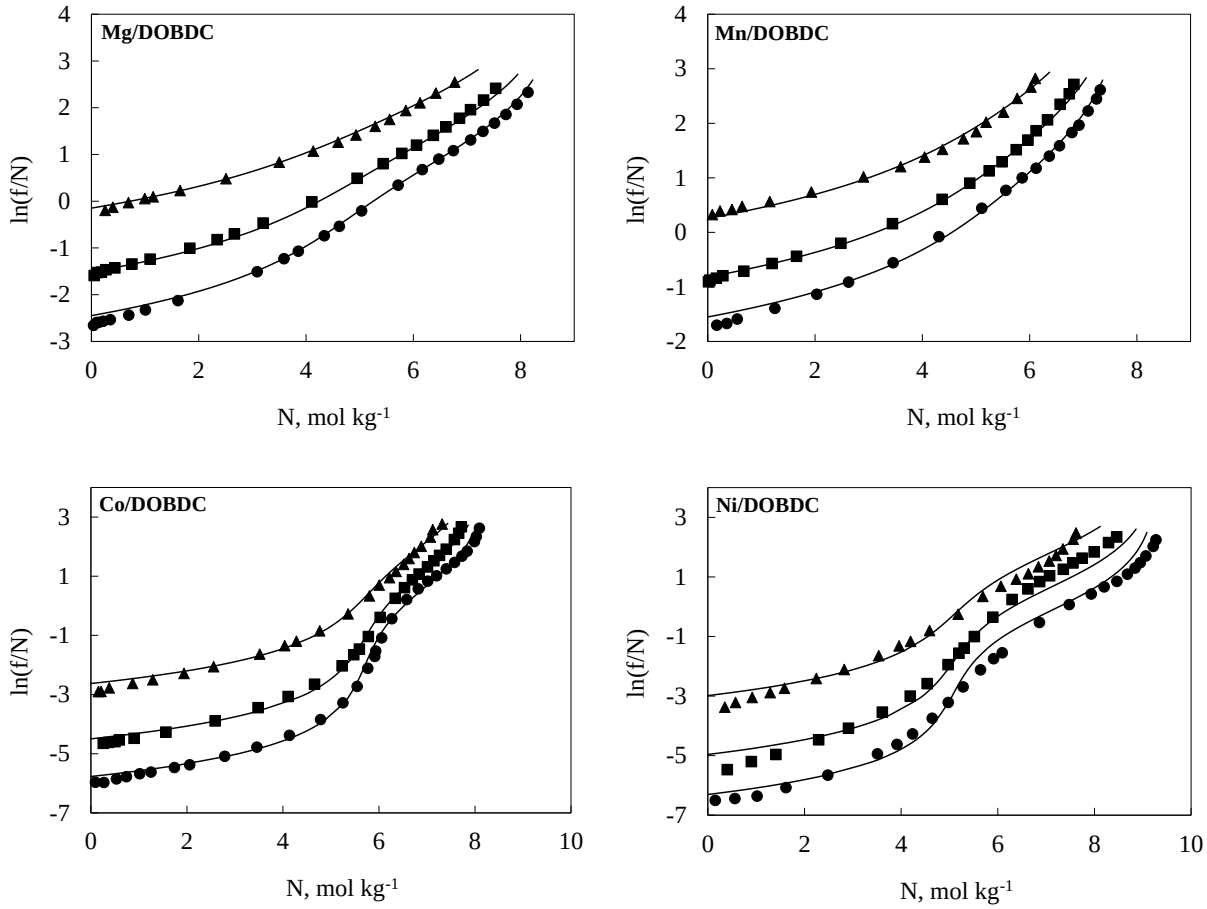

Figure S6. CO isotherms in virial domain. Symbols are experimental data at 294 K (●), 315 K (■) and 352 K (▲); lines are fits obtained using DSL isotherm parameters from Tables S3.

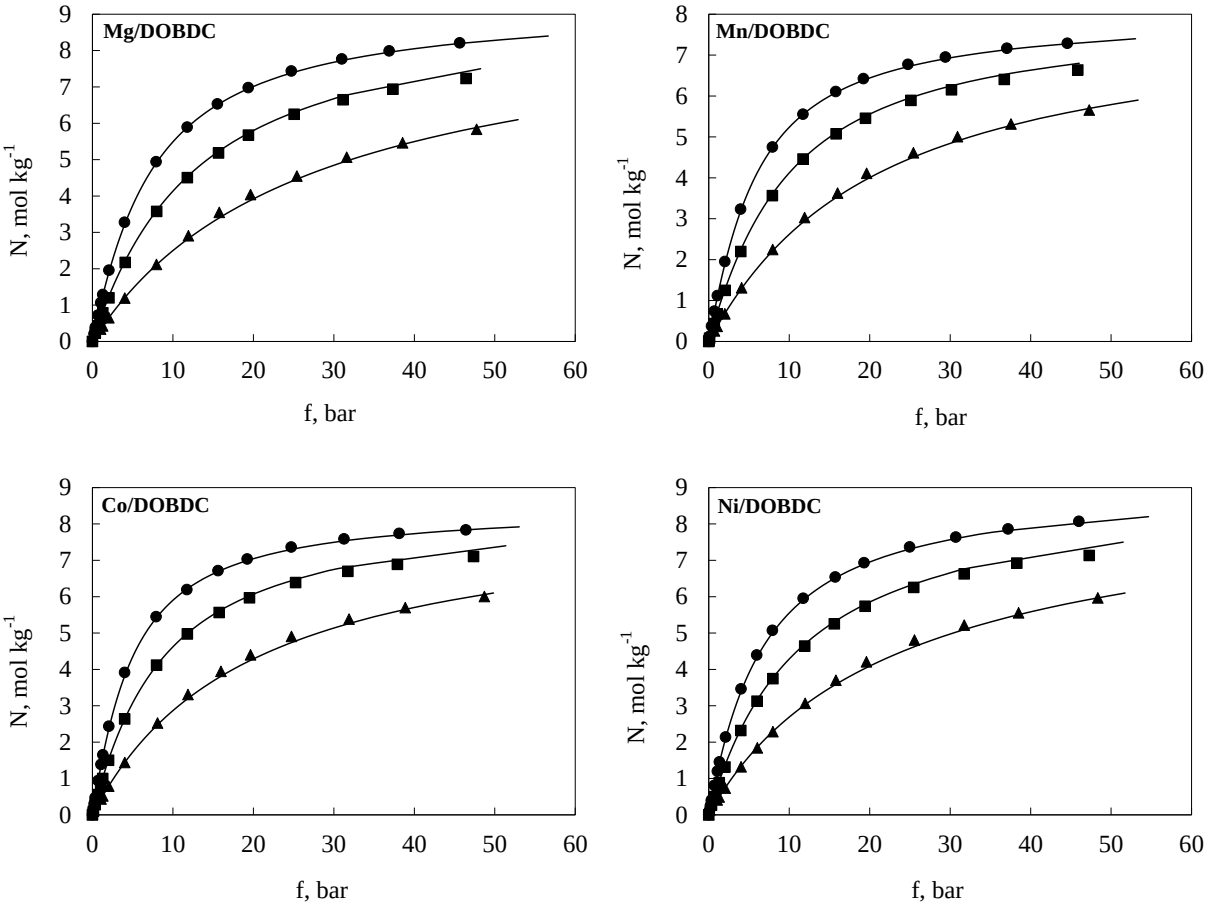

Figure S7. CH_4 isotherms. Symbols are experimental data at 294 K (●), 315 K (■) and 352 K (▲); lines are fits obtained using Langmuir-virial isotherm parameters from Tables S4.

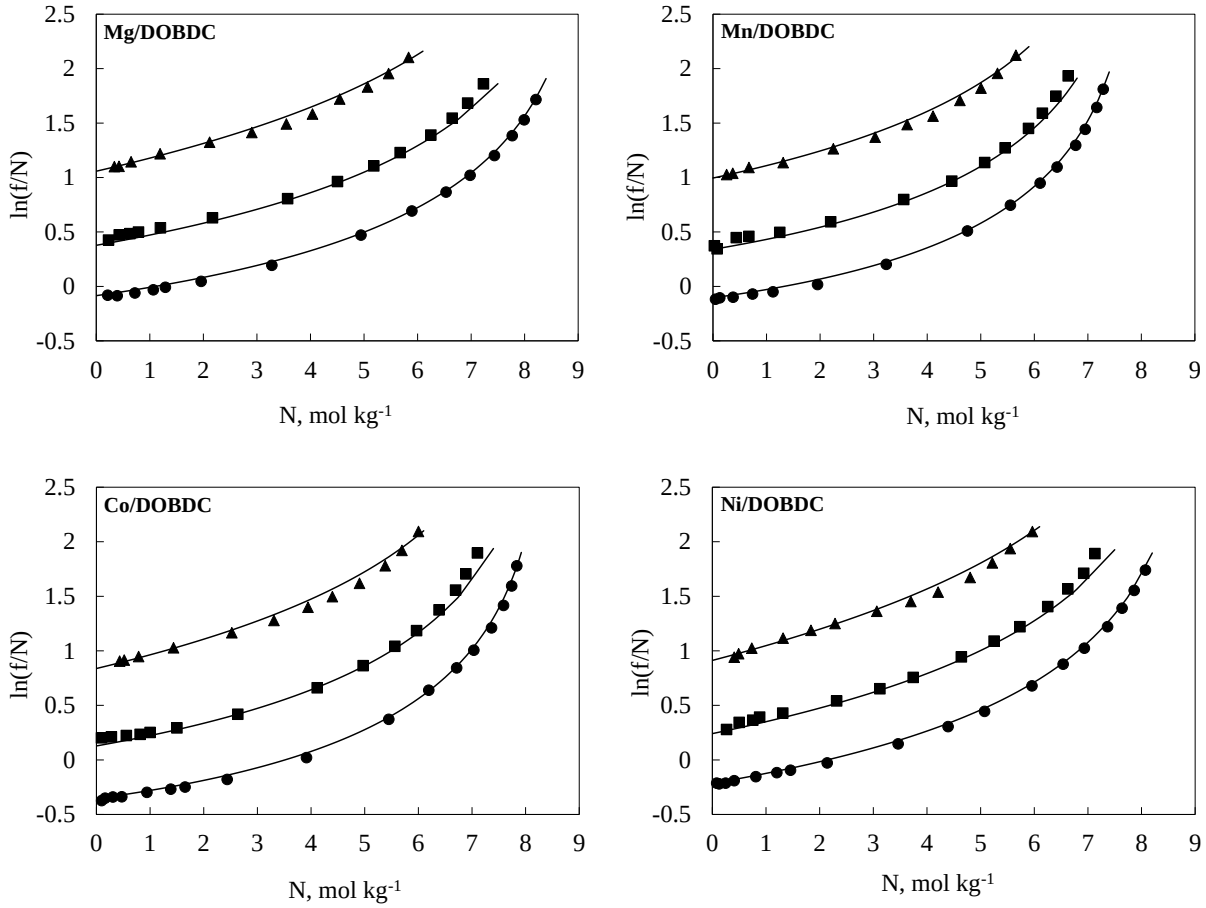

Figure S8. CH_4 isotherms in virial domain. Symbols are experimental data at 294 K (●), 315 K (■) and 352 K (▲); lines are fits obtained using Langmuir-virial isotherm parameters from Tables S4.

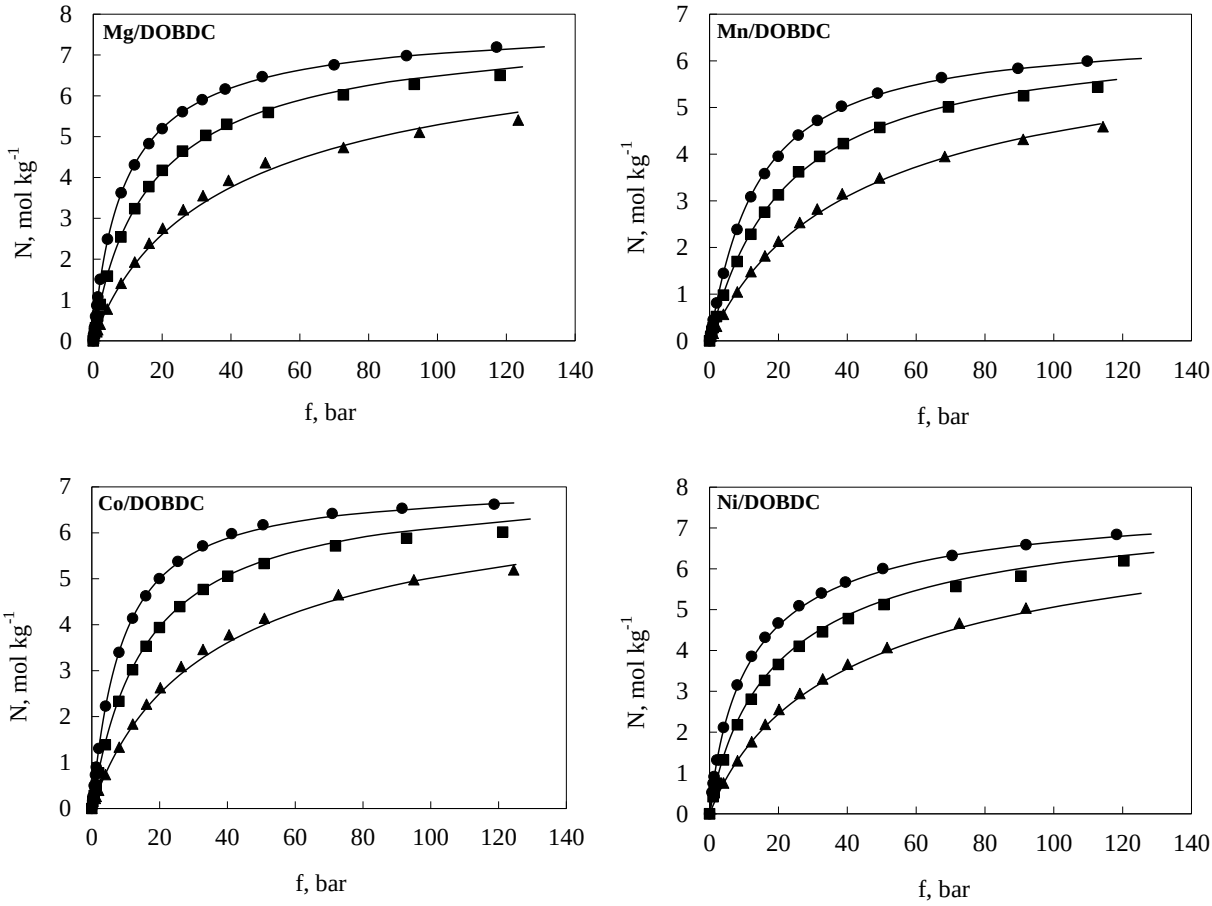

Figure S9. N_2 isotherms. Symbols are experimental data at 294 K (●), 315 K (■) and 352 K (▲); lines are fits obtained using Langmuir-virial isotherm parameters from Tables S5.

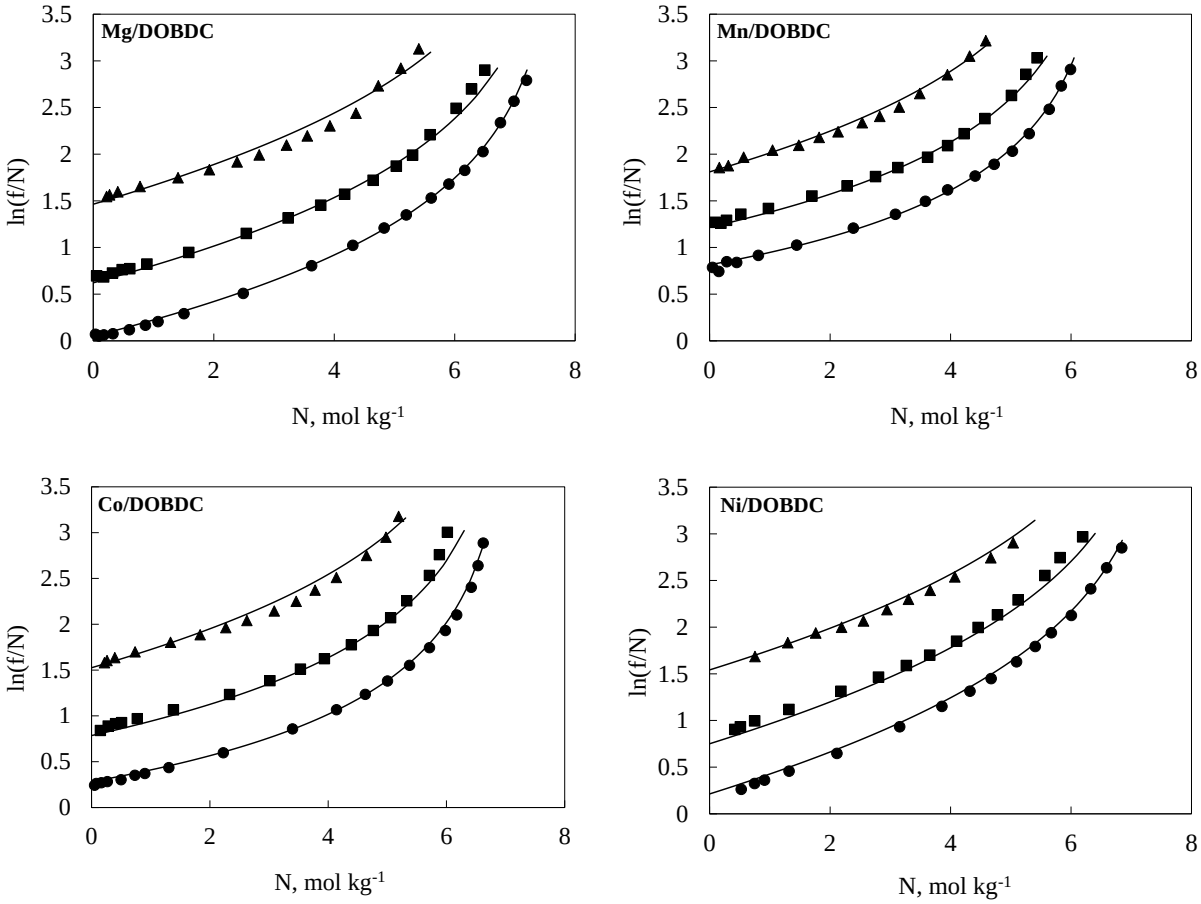

Figure S10. N_2 isotherms in virial domain. Symbols are experimental data at 294 K (●), 315 K (■) and 352 K (▲); lines are fits obtained using Langmuir-virial isotherm parameters from Tables S5.

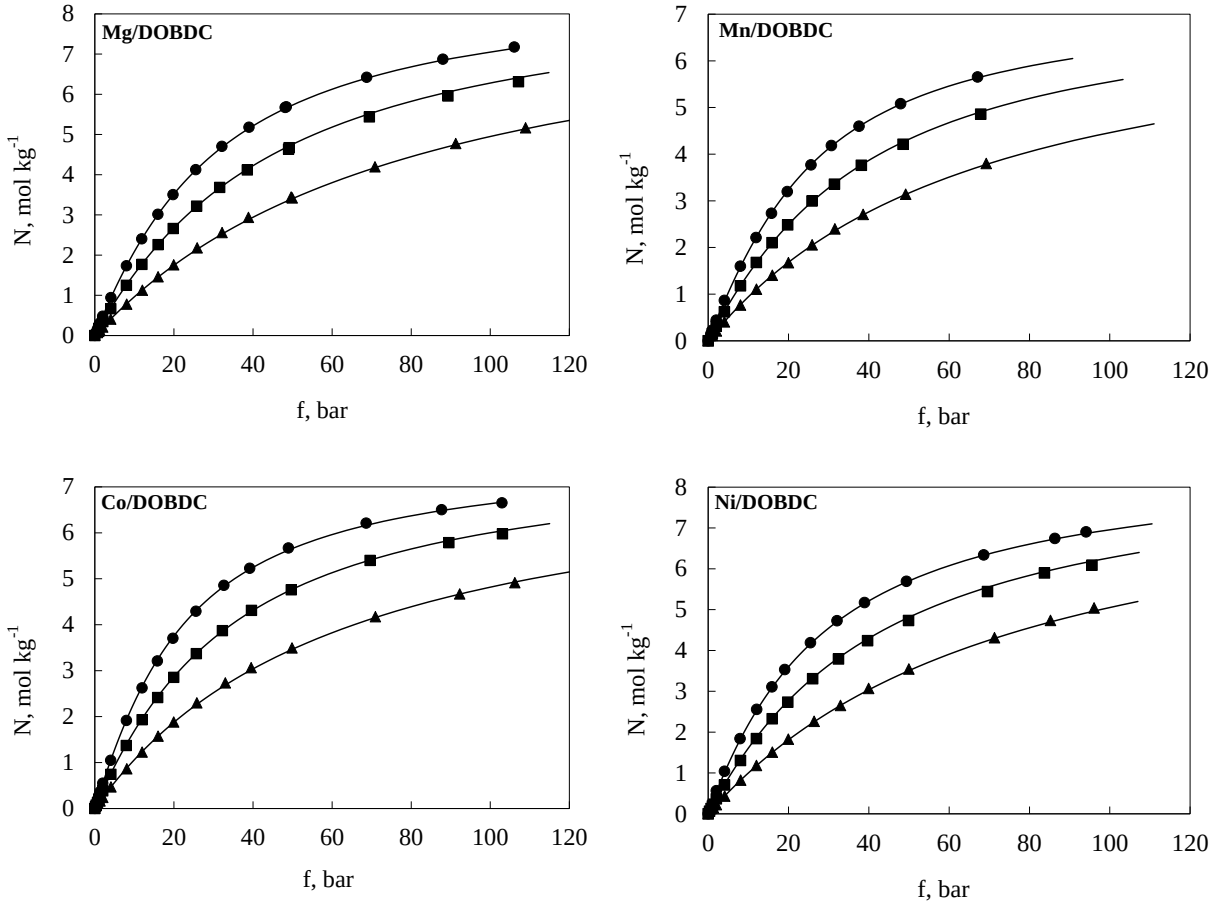

Figure S11. Ar isotherms. Symbols are experimental data at 294 K (●), 315 K (■) and 352 K (▲); lines are fits obtained using Langmuir-virial isotherm parameters from Tables S6.

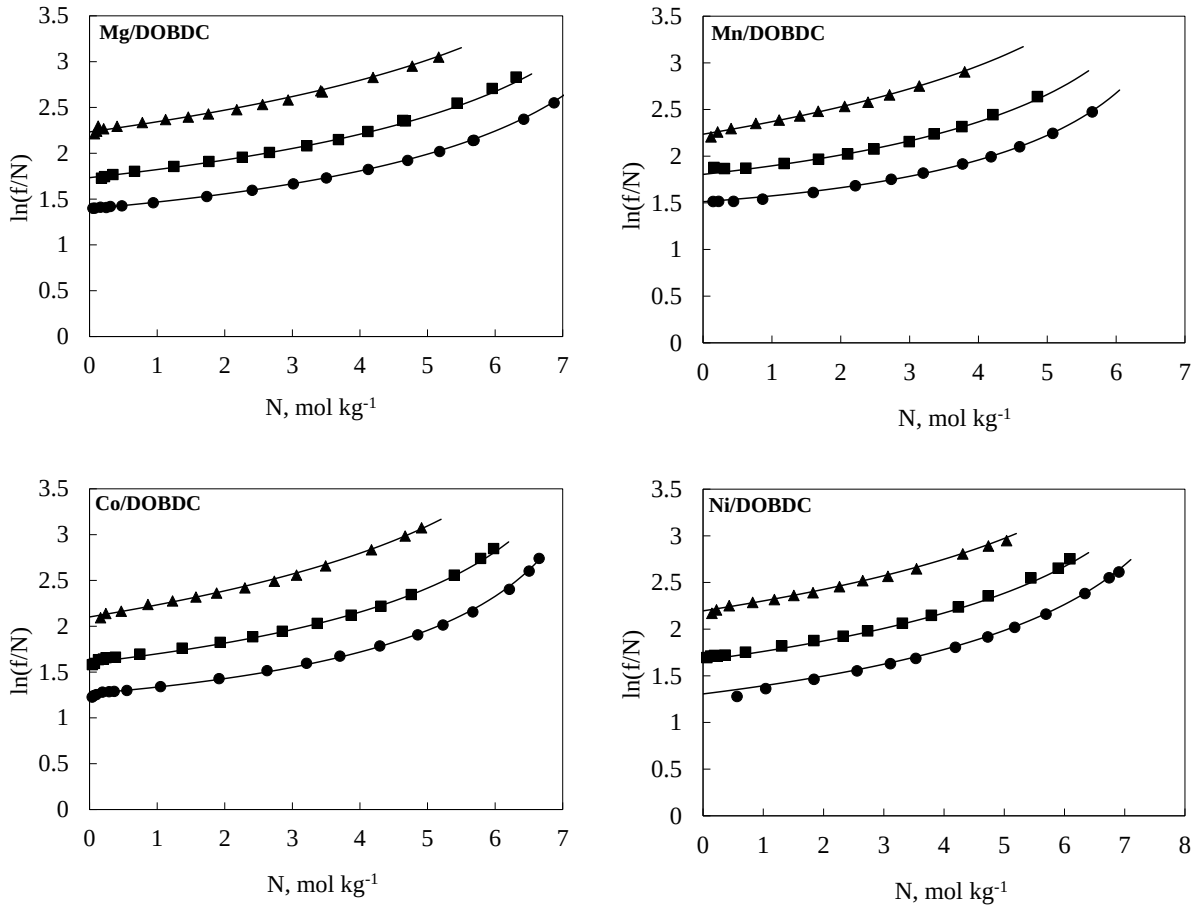

Figure S12. Ar isotherms in virial domain. Symbols are experimental data at 294 K (●), 315 K (■) and 352 K (▲); lines are fits obtained using Langmuir-virial isotherm parameters from Tables S6.

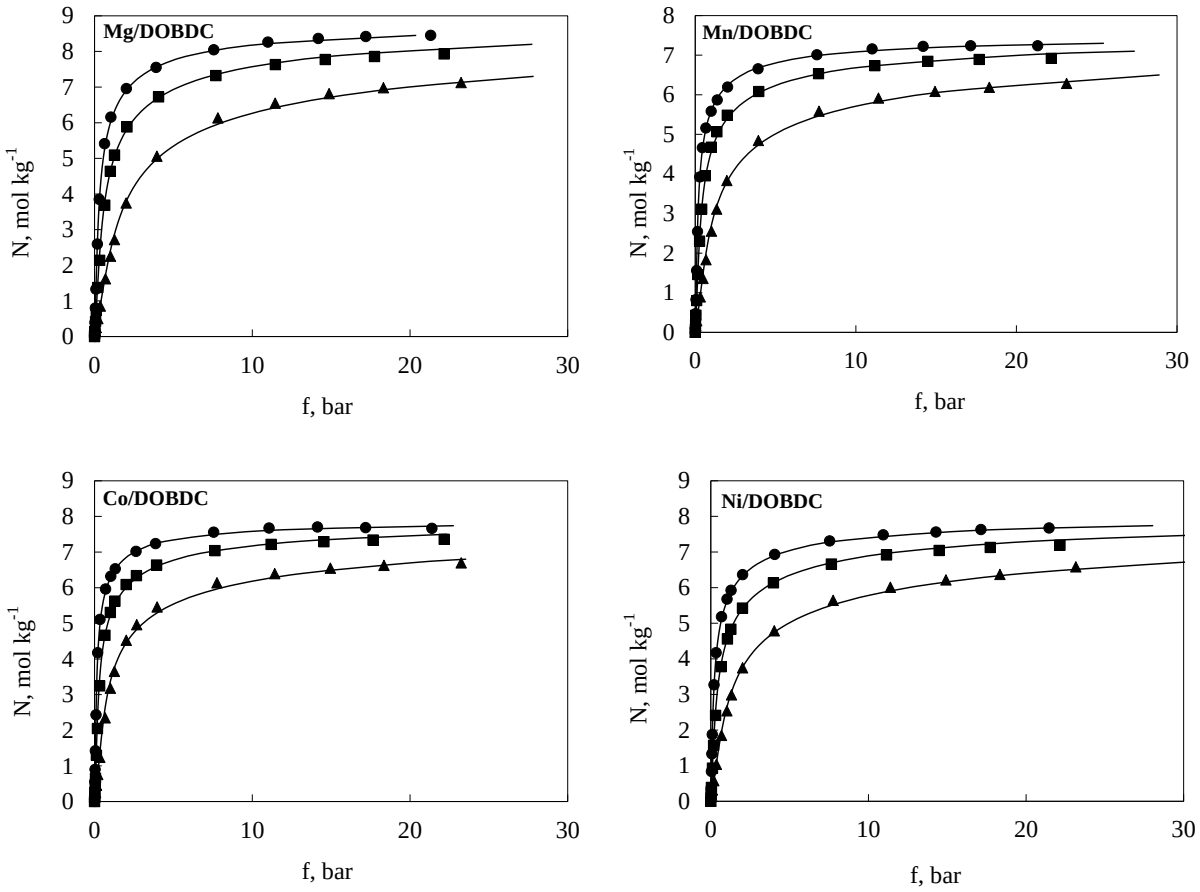

Figure S13. C_2H_6 isotherms. Symbols are experimental data at 294 K (●), 315 K (■) and 352 K (▲); lines are fits obtained using Langmuir-virial isotherm parameters from Tables S7.

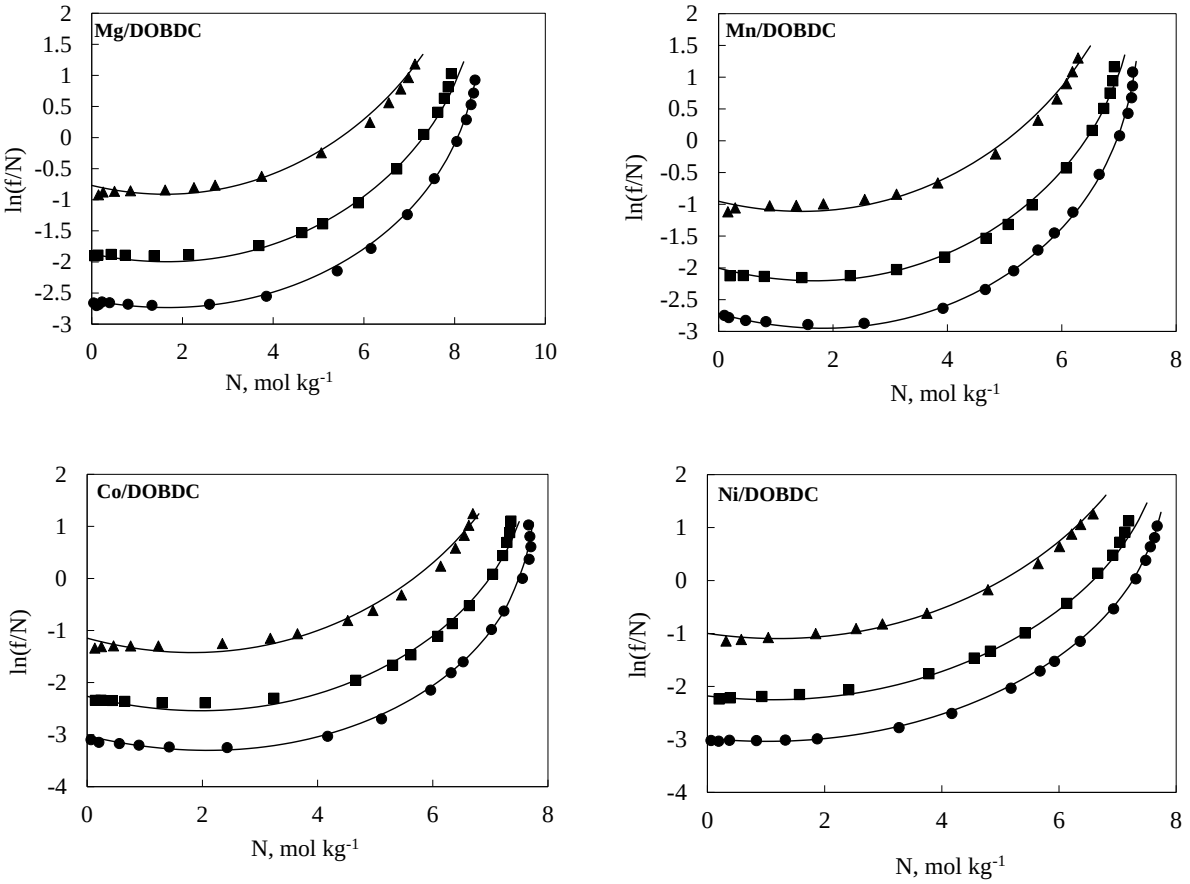

Figure S14. C_2H_6 isotherms in virial domain. Symbols are experimental data at 294 K (●), 315 K (■) and 352 K (▲); lines are fits obtained using Langmuir-virial isotherm parameters from Tables S7.

Variation of Henry's constants (β) and adsorption enthalpy with polarizability

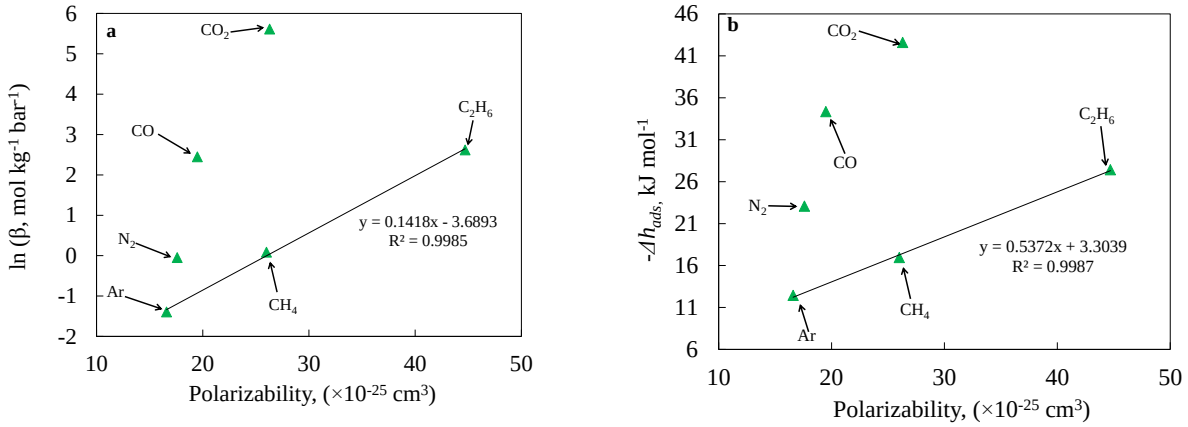

Figure S15. Henry's constant at 294 K (**a**) and enthalpy of adsorption at zero occupancy (**b**) as a function of polarizability of the adsorbate for Mg/DOBDC adsorbent; linear trend lines for non-polar adsorbates are also shown.

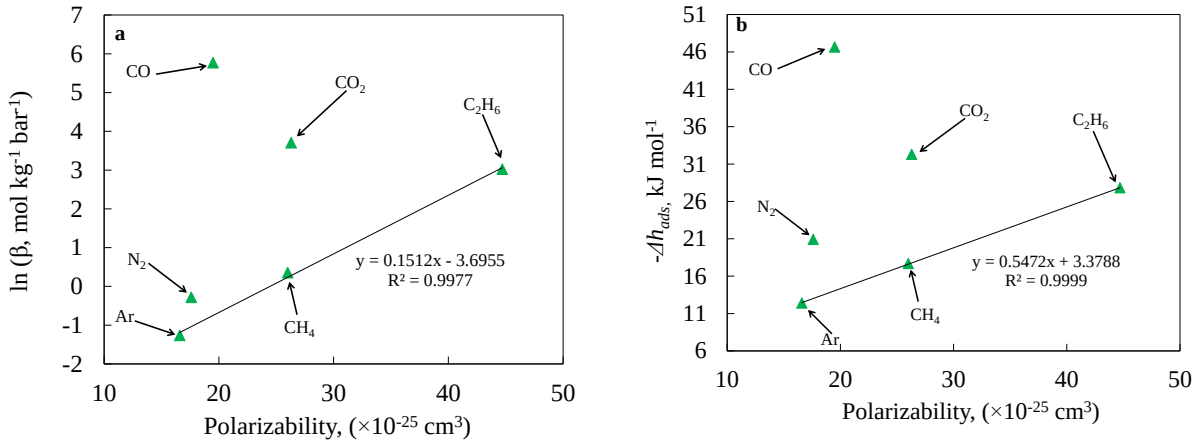

Figure S16. Henry's constant at 294 K (**a**) and enthalpy of adsorption at zero occupancy (**b**) as a function of polarizability of the adsorbate for Co/DOBDC adsorbent; linear trend lines for non-polar adsorbates are also shown.

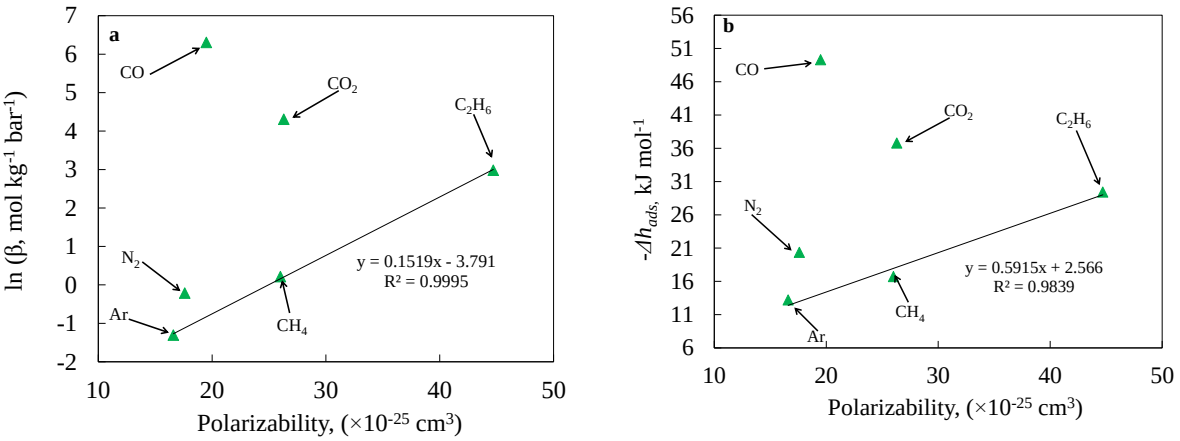

Figure S17. Henry's constant at 294 K (**a**) and enthalpy of adsorption at zero occupancy (**b**) as a function of polarizability of the adsorbate for Ni/DOBDC adsorbent; linear trend lines for non-polar adsorbates are also shown.

Comparison of isotherms of different M/DOBDC samples

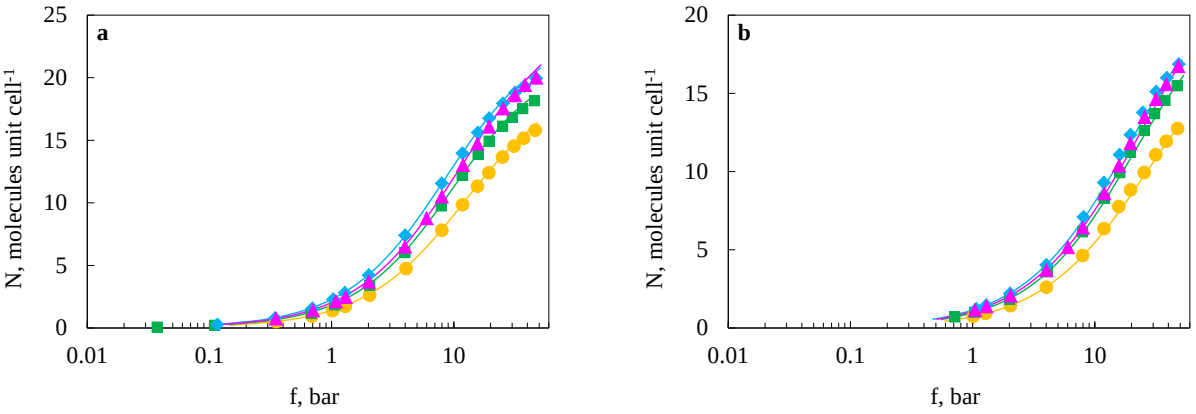

Figure S18. CH_4 isotherms at 315 K **(a)** and 352 K **(b)** on Mg/DOBDC (●), Mn/DOBDC (■), Co/DOBDC (♦) and Ni/DOBDC (▲); symbols are experimental data and lines are fits obtained using Langmuir-virial model parameters from Table S4 in supporting information.

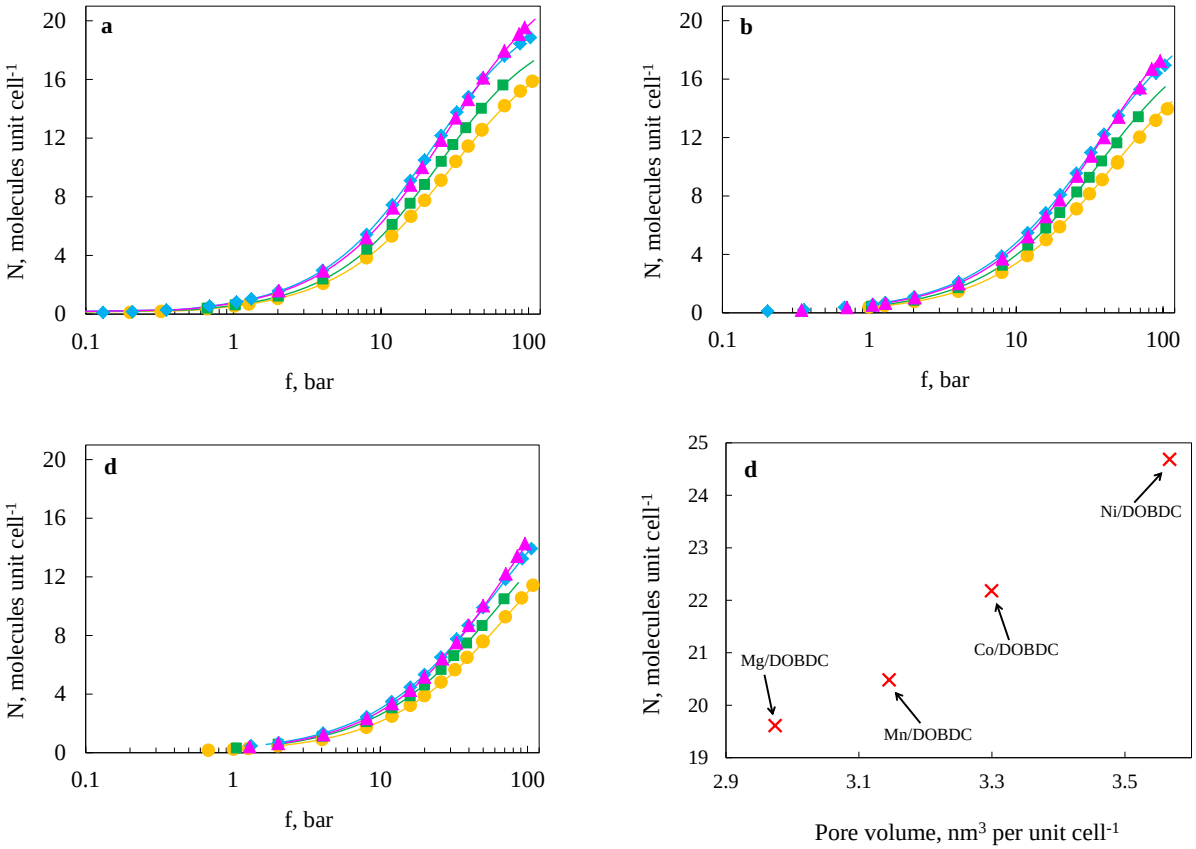

Figure S19. Ar isotherms at 294 K (**a**), 315 K (**b**), and 352 K (**c**) on Mg/DOBDC (●), Mn/DOBDC (■), Co/DOBDC (♦) and Ni/DOBDC (▲). Symbols are experimental data and lines are fits obtained using Langmuir-virial model parameters from Table S6 in supporting information. (b) Variation of saturation uptake with pore volume.

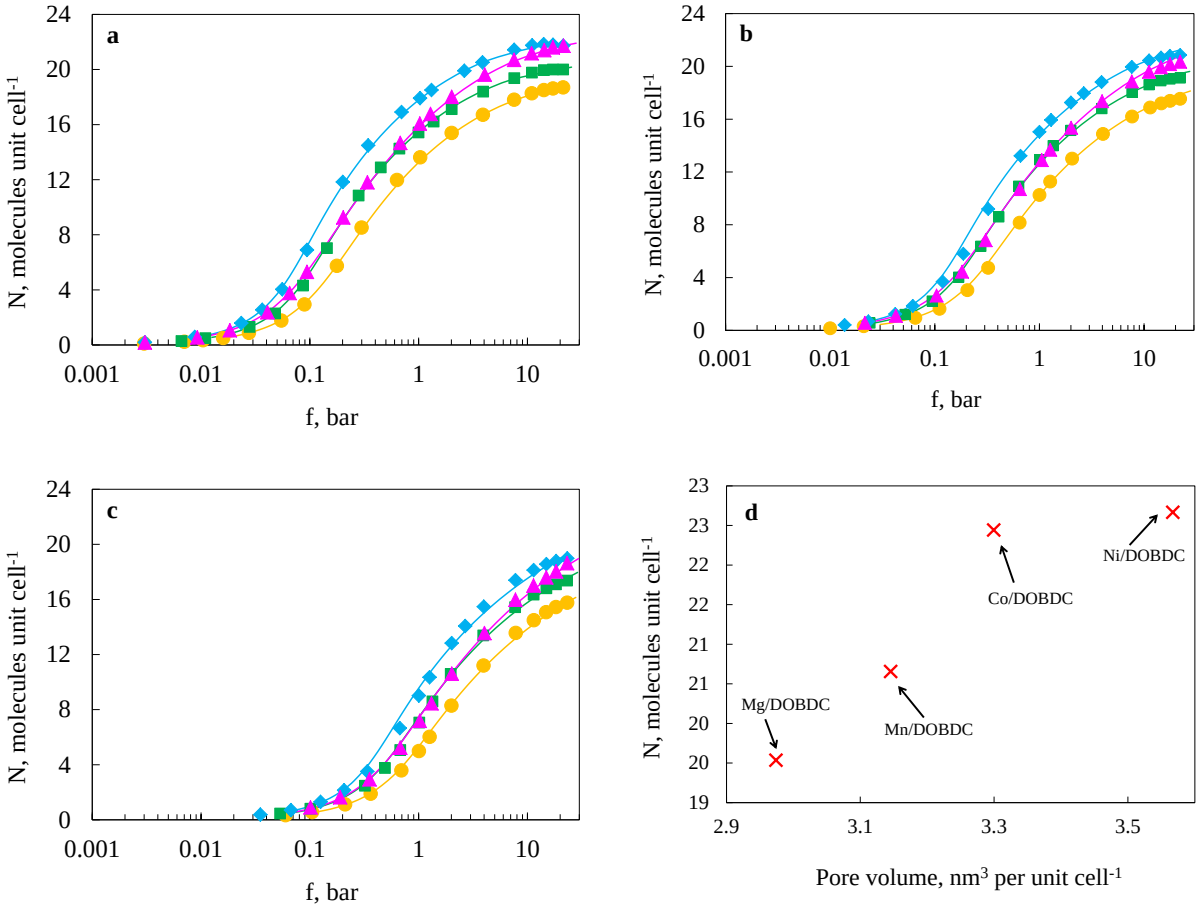

Figure S20. C_2H_6 isotherms at 294 K (**a**), 315 K (**b**), and 352 K (**c**) on Mg/DOBDC (●), Mn/DOBDC (■), Co/DOBDC (♦) and Ni/DOBDC (▲). Symbols are experimental data and lines are fits obtained using Langmuir-virial model parameters from Table S7 in supporting information. (b) Variation of saturation uptake with pore volume.

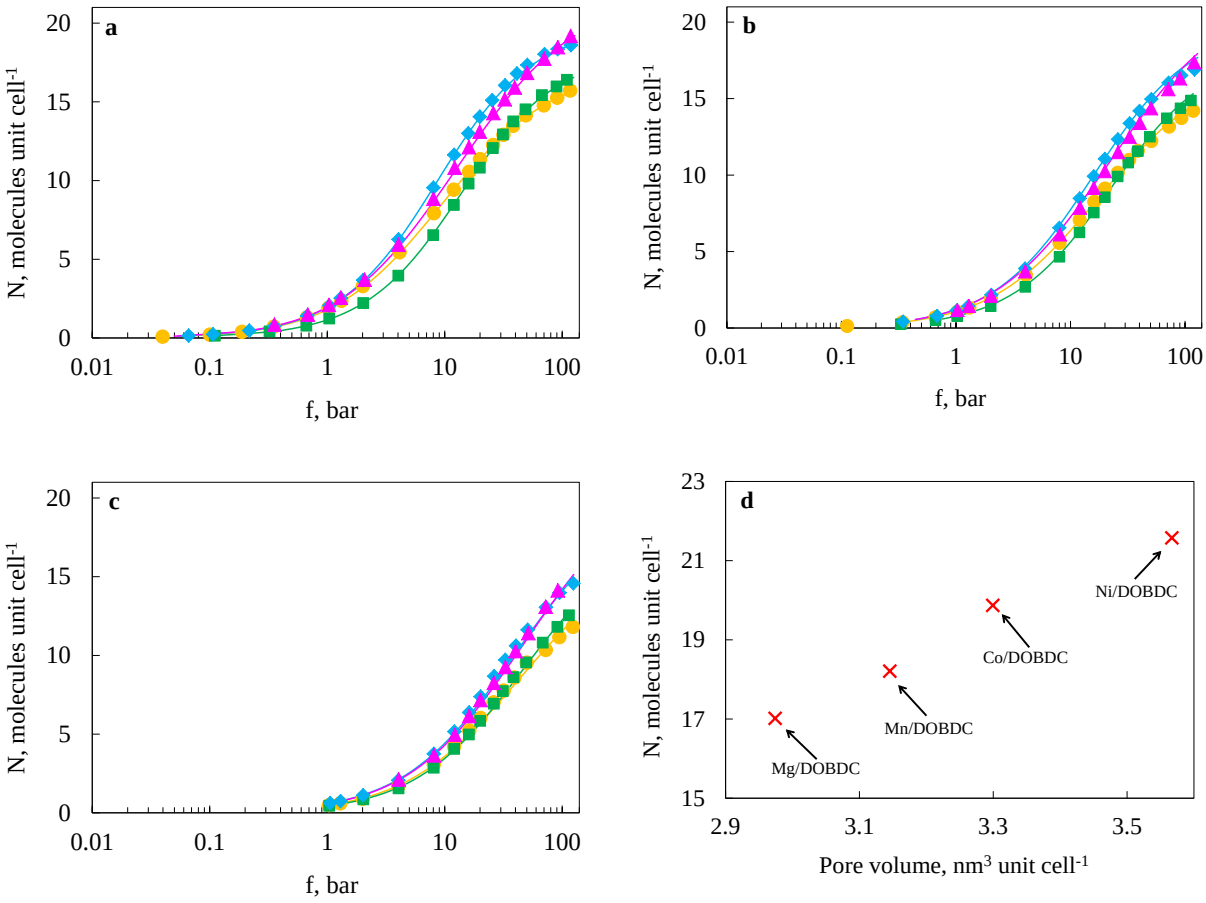

Figure S21. N_2 isotherms at 294 K (**a**), 315 K (**b**), and 352 K (**c**) on Mg/DOBDC (●), Mn/DOBDC (■), Co/DOBDC (♦) and Ni/DOBDC (▲). Symbols are experimental data and lines are fits obtained using Langmuir-virial model parameters from Table S5 in supporting information. (b) Variation of saturation uptake with pore volume.

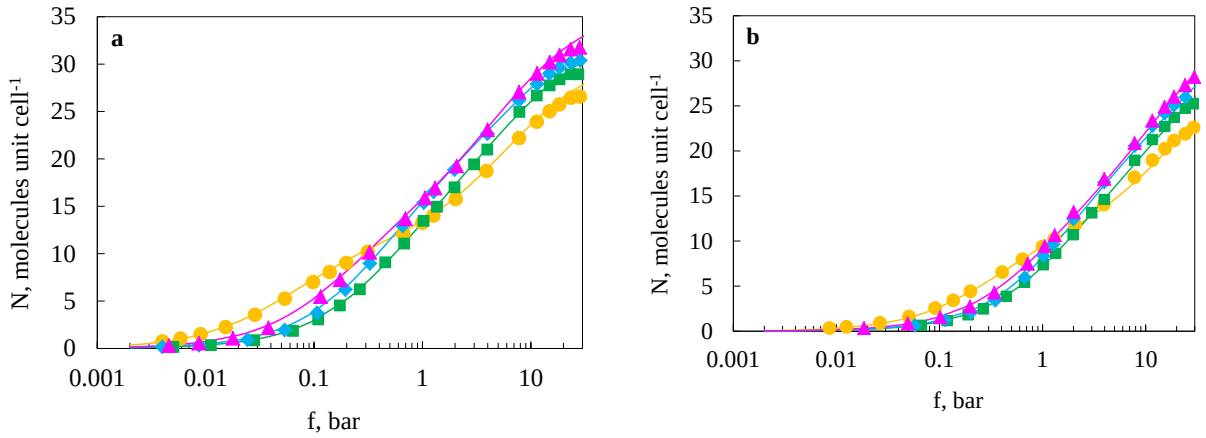

Figure S22. CO_2 isotherms at 315 K **(a)** and 352 K **(b)** on Mg/DOBDC (●), Mn/DOBDC (■), Co/DOBDC (♦) and Ni/DOBDC (▲); symbols are experimental data and lines are fits obtained using DSL model parameters from Table S2 in supporting information.

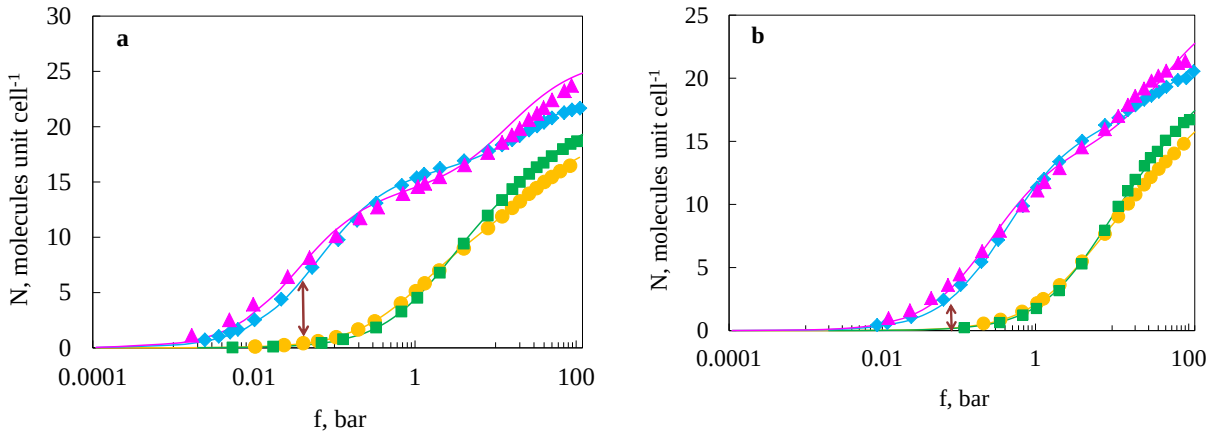

Figure S23. CO isotherms at 315 K **(a)** and 352 K **(b)** on Mg/DOBDC (●), Mn/DOBDC (■), Co/DOBDC (♦) and Ni/DOBDC (▲); symbols are experimental data and lines are fits obtained using DSL model parameters from table S3 in supporting information.

Fit parameters

Table S2. Fit parameters of dual site Langmuir (DSL) isotherm of CO_2

parameters	Mg/DOBDC	Mn/DOBDC	Co/DOBDC	Ni/DOBDC
N_1^{max}, mol kg^{-1}	5.19	6.18	7.00	5.39
N_2^{max}, mol kg^{-1}	9.07	6.06	5.42	7.53
$\beta_1^{(0)} \times 10^5$, bar^{-1}	0.132	3.520	0.964	0.322
$\beta_1^{(1)}$, K	5142.6	3436.8	3901.3	4477.6
$\beta_2^{(0)} \times 10^5$, bar^{-1}	0.239	0.323	0.248	0.805
$\beta_2^{(1)}$, K	3508.2	3385.6	3424.8	3163.0

.

Table S3. Fit parameters of dual site Langmuir (DSL) isotherm of CO

parameters	Mg/DOBDC	Mn/DOBDC	Co/DOBDC	Ni/DOBDC
N_1^{max}, mol kg^{-1}	4.68	5.13	5.70	5.08
N_2^{max}, mol kg^{-1}	4.17	2.74	2.61	4.25
$\beta_1^{(0)} \times 10^5$, bar^{-1}	0.169	1.431	0.029	0.019
$\beta_1^{(1)}$, K	4167.6	3247.5	5611.5	5932.0
$\beta_2^{(0)} \times 10^5$, bar^{-1}	2.502	0.987	1.108	0.116
$\beta_2^{(1)}$, K	2253.7	2447.4	2581.5	3453.2

Table S4. Fit parameters of Langmuir-virial isotherm of CH_4

parameters	Mg/DOBDC	Mn/DOBDC	Co/DOBDC	Ni/DOBDC
$\beta^{(0)}\times 10^3$, mol kg^{-1} bar^{-1}	1.06	1.4	1.02	1.32
$\beta^{(1)}$, K	2039.2	1962.2	2127.2	2010.8
$b^{(0)}$, mol^{-1} kg	0.229	0.176	0.259	0.241
$b^{(1)}$, mol^{-1} kg K	-78.0	-68.2	-91.1	-78.3
N^{max}, mol kg^{-1}	9.33	8.07	8.52	9.10

Table S5. Fit parameters of Langmuir-virial isotherm of N_2

parameters	Mg/DOBDC	Mn/DOBDC	Co/DOBDC	Ni/DOBDC
$\beta^{(0)}\times 10^3$, mol kg^{-1} bar^{-1}	0.18	1.05	0.40	0.25
$\beta^{(1)}$, K	2524.2	1776.9	2218.5	2371
$b^{(0)}$, mol^{-1} kg	0.199	0.393	0.405	0.066
$b^{(1)}$, mol^{-1} kg K	-47.4	-124.3	-126.3	2.5
N^{max}, mol kg^{-1}	7.79	6.66	7.08	7.70

Table S6. Fit parameters of Langmuir-virial isotherm of Ar

parameters	Mg/DOBDC	Mn/DOBDC	Co/DOBDC	Ni/DOBDC
$\beta^{(0)}\times 10^3$, mol kg^{-1} bar^{-1}	1.53	2.74	1.76	1.22
$\beta^{(1)}$, K	1495.2	1290.2	1292.5	1587.9
$b^{(0)}$, mol^{-1} kg	0.183	0.353	0.301	0.082
$b^{(1)}$, mol^{-1} kg K	-67.6	-127.8	-107.9	-34.3
N^{max}, mol kg^{-1}	8.87	7.41	7.82	8.72

Table S7. Fit parameters of Langmuir-virial isotherm of C_2H_6

parameters	Mg/DOBDC	Mn/DOBDC	Co/DOBDC	Ni/DOBDC
$\beta^{(0)}\times 10^3$, mol kg^{-1} bar^{-1}	0.183	0.335	0.235	0.117
$\beta^{(1)}$, K	3298.2	3152.0	3345.2	3538.4
$b^{(0)}$, mol^{-1} kg	-0.472	-0.189	-0.608	-0.557
$b^{(1)}$, mol^{-1} kg K	65.1	-56.7	64.0	95.7
$c^{(0)}$, mol^{-2} kg^2	0.109	0.102	0.170	0.128
$c^{(1)}$, mol^{-2} kg^2 K	-22.4	-13.5	-34.6	-25.1
N^{max}, mol kg^{-1}	8.79	7.47	7.88	7.98

Enthalpy of adsorption

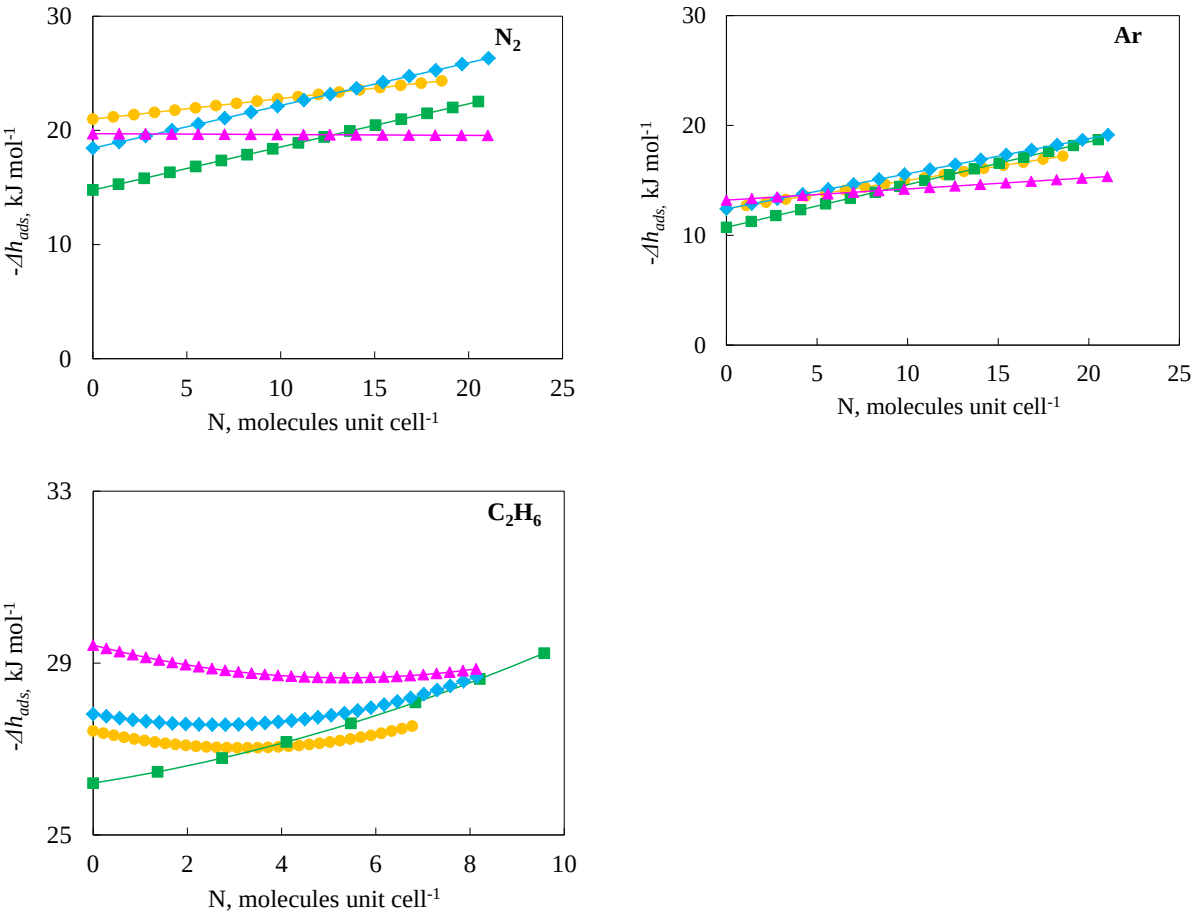

Figure S24. Variation of adsorption enthalpy of with loading for Mg/DOBDC (●), Mn/DOBDC (■), Co/DOBDC (♦) and Ni/DOBDC.

IAST predictions for selectivities at various conditions

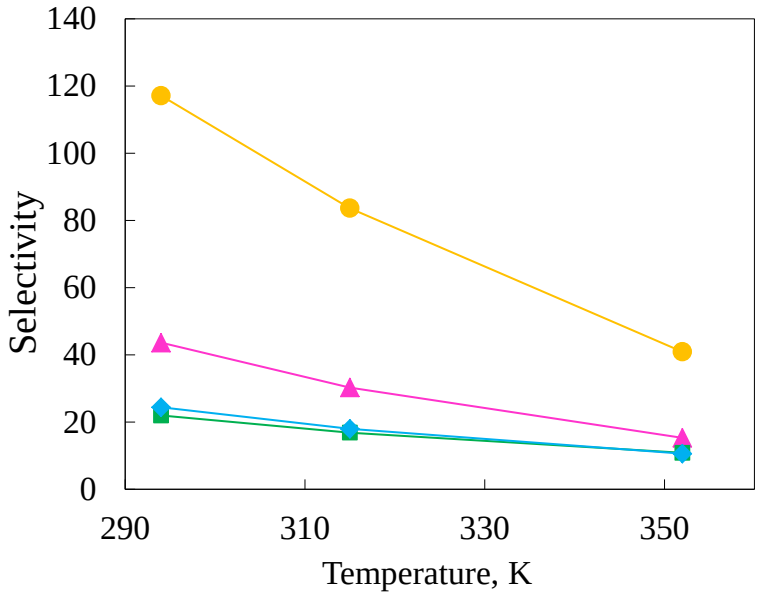

Figure S25. Effect of temperature on CO_2 selectivity (for 20% molar composition of CO_2) over CH_4 at 1 bar total pressure for Mg/DOBDC (●), Mn/DOBDC (■), Co/DOBDC (♦) and Ni/DOBDC (▲). Symbols are calculated values; lines are drawn as a guide to the eyes.

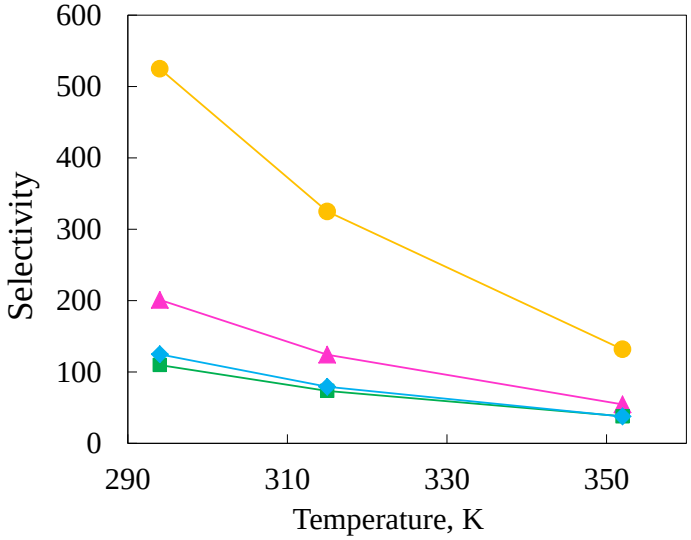

Figure S26. Effect of temperature on CO_2 selectivity (for 20% molar composition of CO_2) over Ar at 1 bar total pressure for Mg/DOBDC (●), Mn/DOBDC (■), Co/DOBDC (♦) and Ni/DOBDC (▲). Symbols are calculated values; lines are drawn as a guide to the eyes.

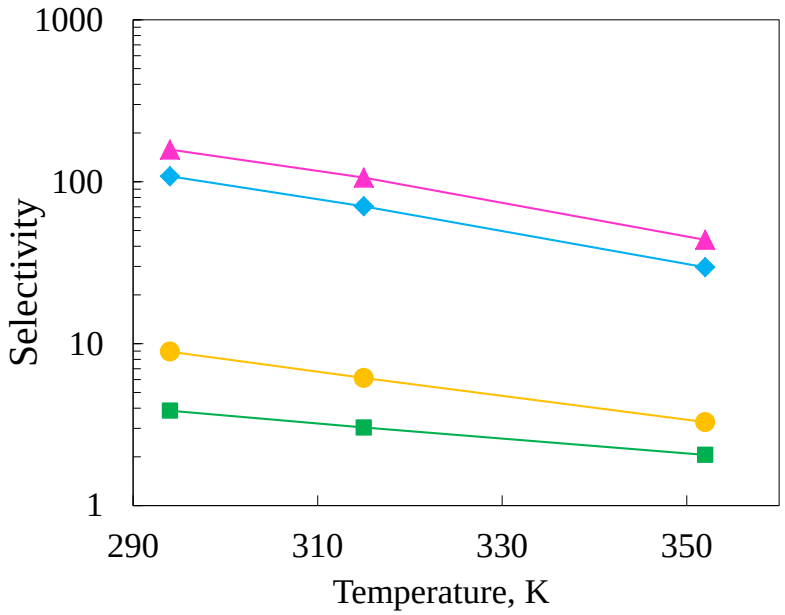

Figure S27. Effect of temperature on CO selectivity (for 20% molar composition of CO) over CH_4 at 1 bar total pressure for Mg/DOBDC (●), Mn/DOBDC (■), Co/DOBDC (♦) and Ni/DOBDC (▲). Symbols are calculated values; lines are drawn as a guide to the eyes.

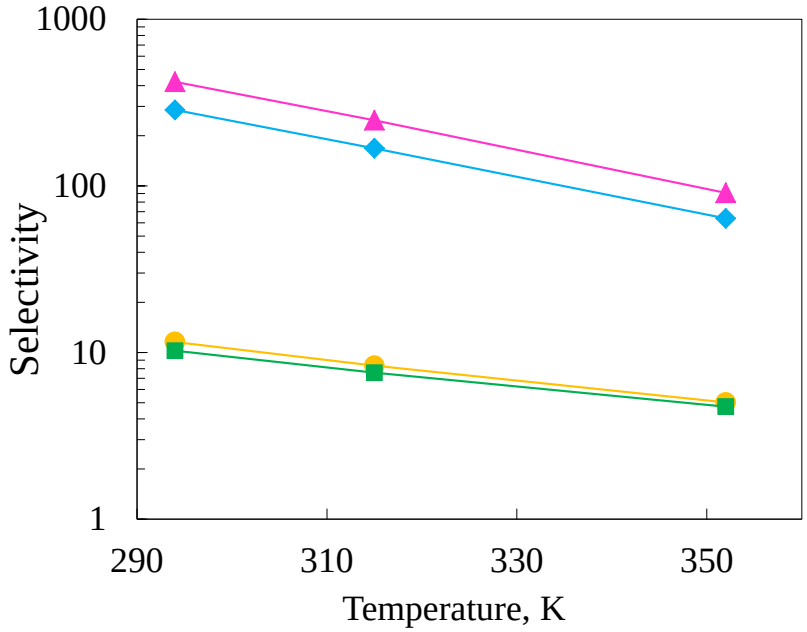

Figure S28. Effect of temperature on CO selectivity (for 20% molar composition of CO) over N_2 at 1 bar total pressure for Mg/DOBDC (●), Mn/DOBDC (■), Co/DOBDC (♦) and Ni/DOBDC (▲). Symbols are calculated values; lines are drawn as a guide to the eyes.

References

(1) Caskey, S. R.; Wong-Foy, A. G.; Matzger, A. J. Dramatic Tuning of Carbon Dioxide Uptake via Metal Substitution in a Coordination Polymer with Cylindrical Pores. *J. Am. Chem. Soc.* **2008,** *130,* 10870–10871.

(2) Zhou, W.; Wu, H.; Yildirim, T. Enhanced H_2 Adsorption in Isostructural Metal Organic Frameworks with Open Metal Sites: Strong Dependence of the Binding Strength on Metal Ions. *J. Am. Chem. Soc.* **2008,** *130,* 15268–15269.

(3) Dietzel, P. D. C.; Besikiotis, V.; Blom, R. Application of metal–organic frameworks with coordinatively unsaturated metal sites in storage and separation of methane and carbon dioxide. *J. Mater. Chem.* **2009,** *19,* 7362–7370.